Multiple Strata of Exponentially Growing Polyelectrolyte Multilayer Films

Laurent Jourdainne,[†,‡] Youri Arntz,[†,‡] Bernard Senger,[†,‡] Christian Debry,[†,⊥] Jean-Claude Voegel,[†,‡] Pierre Schaaf,[§] and Philippe Lavalle*[,†,‡]

Institut National de la Santé et de la Recherche Médicale, Unité 595, 11 rue Humann, 67085 Strasbourg Cedex, France, Faculté de Chirurgie Dentaire, Université Louis Pasteur, 1 Place de l'Hôpital, 67000 Strasbourg, France, Centre National de la Recherche Scientifique, UPR22, Institut Charles Sadron, 6 rue Boussingault, 67083 Strasbourg Cedex, France, and Department of Otolaryngology-Head and Neck Surgery, Hautepierre Hospital, Avenue Molière, BP49 67098 Strasbourg Cedex, France

Received September 21, 2006; Revised Manuscript Received October 30, 2006

ABSTRACT: Polyelectrolyte multilayers are potential candidates for bioactive coatings with time scheduled biological activity. One way to achieve this goal is to use coatings constituted of several successive multilayers. We demonstrate in the present study that the buildup of successively two exponentially growing multilayers, namely a poly(L-lysine)/poly(L-glutamic acid) $(PLL/PGA)_n$ film on top of a poly(L-lysine)/hyaluronic acid $(PLL/HA)_m$ precursor film is possible. The growth process of $(PLL/PGA)_n$ remains exponential and the presence of the underneath $(PLL/HA)_m$ multilayers enhances the film growth when compared with a $(PLL/PGA)_n$ film constructed on a solid substrate. PGA also diffuses into the entire $(PLL/HA)_m$ multilayer and forms complexes with free PLL chains present in the precursor architecture. As the buildup of $(PLL/PGA)_n$ progresses, the PLL chains deposited on top of the film loose gradually their ability to diffuse into the $(PLL/HA)_m$ film. These results should have far reaching consequences on the buildup of multistrata films presenting biological activity.

Introduction

The deposition of polyelectrolyte multilayer (PEM) films through the layer by layer method (LBL) has stimulated a tremendous amount of studies since 10 years.[1,2] Iler in 1966 still described the formation of layer-by-layer structures using anionic and cationic colloidal particles.[3] Some of the physicochemical mechanisms responsible for these self-assembling structures have been described in details. The development of numerous potential applications is now in progress.[4−15] The buildup of PEM films occurs through the alternate dipping of a substrate in polyanion and polycation solutions and is most often the consequence of strong electrostatic interactions between the two constituting partners. This kind of surface self-assembly offers new opportunities in the modification of surfaces, since it constitutes a versatile technique applicable to any kind of materials carrying initially a surface charge. Moreover, it is possible to control deposited film thickness, roughness, porosity, mechanical properties by changing the nature of the polyelectrolytes, the number of layers deposited, the pH and ionic strength of the solutions from which polyelectrolytes are adsorbed.[16−21] Two kinds of growing mechanisms for these PEM films have been described: (i) a well-known linear growth regime in which the thickness and the amount of polyelectrolytes deposited per bilayer increase linearly with the number of deposited bilayers, n,[18,22] and (ii) an exponential growth in which the thickness and the amount adsorbed increase exponentially with n.[23−28] Multilayers composed of synthetic polyelectrolytes like poly(allylamine)/poly(styrenesulfonate) or poly(diallyldimethylammonium)/poly(styrenesulfonate) constitute typical examples of such linear growth regime systems. These films present a stratified structure, each polyelectrolyte layer interpenetrating only the neighboring ones and the thickness reached after deposition of 10 bilayers is typically on the order of 50 to 100 nm. On the other hand, exponentially growing multilayers concern most of the time natural polyelectrolytes like polyamino acids (poly(glutamic acid), poly(lysine), poly(aspartic acid), ...),[25,29] or polysaccharides (alginate, hyaluronic acid, chitosan, chondroitin sulfate, ...).[23,24]

The exponential growth mechanism of some PEM films was first attributed to the increase of surface roughness with the number of deposited layers.[19,27] However, for systems like poly(L-lysine)/hyaluronic acid (PLL/HA), it was shown that this growth process is related to the ability of at least one of the two polyelectrolytes constituting the film to diffuse "in" and "out" of the whole structure during each bilayer deposition step. In the example of PLL/HA multilayers, it was shown that PLL is the diffusing species.[24,30] The contact of the PLL solution with the film leads to adsorption of a PLL layer on top of the film. Then, a fraction of PLL chains diffuse through the film and are free to move in the structure.[31] After contact with HA, most of the remaining "free" PLL chains in the films also diffuse out of it. As they reach the film/solution interface they form complexes with the incoming HA chains. These complexes constitute the new outer PLL/HA layer at the film/bulk interface. The amount of "free" PLL chains that can diffuse out of the film during the contact with the HA solution is proportional to the film thickness. The amount of PLL/HA complexes formed during this step is also proportional to the film thickness. This finally explains why the buildup follows an exponential growth.

* Corresponding author. Address: INSERM Unité 595, 11 rue Humann, 67085 Strasbourg Cedex, France. Telephone: +33 (0)3 90 24 30 61. Fax: +33 (0)3 90 24 33 79. E-mail: philippe.lavalle@medecine.u-strasbg.fr.

† Institut National de la Santé et de la Recherche Médicale, Unité 595.

‡ Faculté de Chirurgie Dentaire, Université Louis Pasteur.

§ Centre National de la Recherche Scientifique, UPR22, Institut Charles Sadron.

⊥ Department of Otolaryngology-Head and Neck Surgery, Hautepierre Hospital.

10.1021/ma062201e CCC: $37.00
Published on Web 12/19/2006

More recently, it was clearly proven that poly(L-lysine)/poly(L-glutamic acid) (PLL/PGA) multilayers constitute another example of exponentially growing systems.[32] These multilayers can act as a reservoir allowing for the free diffusion of biomolecules before their eventual internalization by cells seeded on the films.[33,34]

PEM films are potential candidates for bioactive coatings presenting time scheduled biological activity. One way to achieve this goal is to use coatings constituted of several successive multilayers. The deposition of a $(C/D)_n$ multilayer on top of a $(A/B)_m$ precursor multilayer can eventually modify the properties of the underlying $(A/B)_m$ film. This may have important consequences for the biological activity of the film. A first step toward multicompartment films was achieved recently by alternating exponentially growing multilayers acting as a compartment for PLL chains and linearly growing films acting as a barrier toward diffusion of PLL.[35] The compartments or reservoirs consisted in exponentially growing PLL/HA multilayers in which some PLL chains diffuse freely. These compartments were delimited by $(\text{poly(allylamine)/poly(styrene-sulfonate)})_{30}$ barriers. Such barriers can separate two compartments and prevent the diffusion of PLL chains from one compartment to the neighboring one. However, we recently demonstrated that such barriers made of synthetic polyelectrolytes (PSS and PAH) act as nondegradable barriers despite the presence of monocytic cells characterized by their great phagocytosis capacity. Thus, cells coming in contact with the film will never be activated by biomolecules located in the underlying compartment. A first strategy to develop degradable barriers using a hydrolyzable polyester was more recently proposed.[36] However the design of such films is far away from the simple layer by layer deposition method.

In the present study, we investigated the buildup of an exponentially growing $(PLL/PGA)_n$ multilayer film on top of another exponentially growing multilayer film made of PLL and HA. We focus especially on how the $(PLL/PGA)_n$ multilayer modifies the properties of the underneath $(PLL/HA)_m$ architecture. When built individually, both films grow exponentially. We find that this remains true for $(PLL/PGA)_n$ built onto a $(PLL/HA)_m$ multilayer film. We will also demonstrate that the deposition of the $(PLL/PGA)_n$ multilayer film on the $(PLL/HA)_m$ film greatly affects the structure of the underneath film. In particular, PGA chains diffuse into the $(PLL/HA)_m$ multilayer film and form complexes with the free PLL chains. These complexes greatly affect the diffusion ability of the chains in the underneath film. These results will be of great importance for the design of multicompartment films and should be of wide use to design multicompartment PEM films with degradable barriers made of poly(amino acid) multilayers and able to deliver sequentially specific biomolecules for surrounding cells.

Experimental Section

Materials. Poly(L-lysine) (PLL, $M_w = 5.89 \times 10^4$ Da) and poly(L-glutamic acid) (PGA, $M_w = 9.78 \times 10^4$ Da) were purchased from Sigma (St. Quentin Fallavier, France). Hyaluronic acid (HA, $M_w = 4.0 \times 10^5$ Da) was obtained from BioIberica (Barcelona, Spain). Polyelectrolyte solutions (1 mg·mL^{-1}) were prepared by dissolution of the adequate amounts of polyelectrolytes in 0.15 M NaCl aqueous solution, pH = 5.9.

Fluorescently Labeled Polyelectrolytes. Fluorescein isothiocyanate (FITC) labeled poly(L-lysine) (PLL^{FITC}, $M_w = 6.67 \times 10^4$ Da) was obtained from Sigma (St. Quentin Fallavier, France). Rhodamine Red-X succinimidyl ester (Invitrogen, France) (Invitrogen, Cergy Pontoise, France) was coupled to PLL as described previously.[37] An appropriate amount of PLL (1 mg·mL^{-1}) was dissolved in a Na_2CO_3 solution (0.1 M, pH = 8.5). Rhodamine (Rho) at 2 mg·mL^{-1} was dissolved in DMSO (dimethyl sulfoxide). We used a ratio of 1 mg of rhodamine for 50 mg of PLL. The solutions were gently mixed at room temperature during 2 h. PLL^{Rho} was purified by dialysis during 3 days. Then the absence of free rhodamine in the solution was checked by UV spectroscopy.

The PGA chains were labeled with the Alexa Fluor 594 probe (Invitrogen), emitting at 609 nm (red), leading to PGA^{AF}. The synthesis of the labeled polyelectrolyte was achieved by coupling PGA with Alexa Fluor 594 hydrazide as described in details elsewhere.[32] The average grafting rate was measured by UV spectrophotometry and was found to be about 1.1 unit per polymer chain.

Buildup of Polyelectrolyte Multilayer Films. The PEM films were built with an automatized dipping robot (Riegler & Kirstein GmbH, Berlin, Germany) on silica slides. The slides were first dipped in a polycation solution for 10 min. Then, a rinsing step was performed by dipping the substrates for 10 min in 0.15 M NaCl solution. The polyanion was then deposited in the same manner. The buildup process was pursued by the alternated deposition of polycations and polyanions. After deposition of n bilayers, the film is denoted $(\text{polycation/polyanion})_n$.

Confocal Laser Scanning Microscopy (CLSM). CLSM observations and FRAP experiments were carried out with a Zeiss LSM 510 microscope using a ×40/1.4 oil immersion objective and with 0.4 μm z-section intervals. FITC fluorescence was detected after excitation at 488 nm with cutoff dichroic mirror 488 nm and emission band-pass filter 505−530 nm (green). Rhodamine fluorescence was detected after excitation at 543 nm, dichroic mirror at 543 nm, and emission long pass filter at 585 nm (red). On the average, four images in the same location were acquired at 512 × 512 pixels. In FRAP experiments, typical bleaching procedure consisted in scanning 50 times a defined area on the scan zone to bleach with a laser power of 30%. The total bleach time reached 10 s. Immediately after the bleach procedure, the first image in the same zone was scanned to control the efficiency of the bleach. Then after given times, new images were taken to follow fluorescence recovery. All the experiments were performed under liquid conditions (NaCl 0.15 M, pH = 5.9).

Quartz Crystal Microbalance (QCM) Measurements. The construction of some PEM films was monitored in situ by quartz crystal microbalance using the axial flow chamber QAFC 302 (QCM-D, D300, Q-Sense, Götenborg, Sweden). The QCM technique consists in measuring of the resonance frequency changes (Δf) of a quartz crystal induced by polyelectrolyte adsorption on the crystal, when compared to the crystal in contact with a 0.15 M NaCl solution. The quartz crystal is excited at its fundamental frequency (5 MHz), and the measurements are performed at the first, third, fifth and seventh overtones (denoted as $\nu = 1$, 3, 5 and 7, respectively) corresponding to 5, 15, 25, and 35 MHz, respectively. Changes in the resonance frequencies, Δf, and in the relaxation of the vibration once the excitation is switched off are measured at these four frequencies. The relaxation measurement gives also access to the change in the dissipation factor, D, of the vibration energy stored in the resonator. The crystal used here is coated with a ≈50 nm SiO_2 film. The measurement methodology has been addressed in details elsewhere.[38] A 0.15 M NaCl solution was injected into the measurement cell by gravity. After stabilization of the signals, 500 μL of PLL solution was injected, left in the cell for 10 min, and rinsed for 10 min with the 0.15 M NaCl solution. During the whole process, the Δf shift was continuously recorded as a function of time. The same procedure was used for the deposition of polyanions (HA or PGA) by adding 500 μL of the solution. The construction was pursued by alternate depositions of PLL and the polyanions. A positive shift in the opposite of the normalized frequency shift, $-\Delta f/\nu$, can be associated, in first approximation, with an increase of the mass adsorbed to the crystal. However, the experimental data ($\Delta f/\nu$ and ΔD) can be analyzed in the framework developed by Voinova et al.[39] Under the hypothesis that the film is a homogeneous and isotropic viscoelastic layer, a thickness value, d, is derived from $\Delta f/\nu$ and ΔD values correspond-

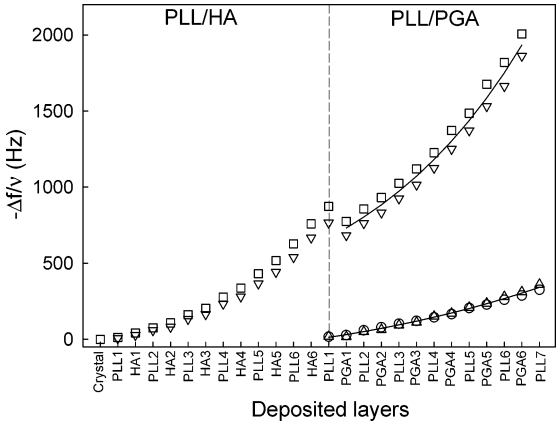

Figure 1. QCM measurements monitoring the changes in the frequency shifts $-\Delta f/\nu$ during the buildup of PLL/PGA multilayer films. Symbols △ and ○ correspond to two independent experiments consisting in the deposition of $(PLL/PGA)_7$ films on a bare crystal. Symbols □ and ▽ correspond to two independent measurements of the buildup of a $(PGA/PLL)_6/PLL$ stratum on a $(PLL/HA)_6/PLL$ precursor stratum. The mean fit of the growths of the $(PGA/PLL)_6/PLL$ films deposited on the $(PLL/HA)_6/PLL$ precursor films with an exponential law of the type $-\Delta f/\nu = a + be^{ck}$ (where k corresponds to the number of deposited layers) leads to the parameter b equal to 612.0 and to the parameter c equal to 0.102 (see the black line corresponding to the mean fit). The fits for the $(PLL/PGA)_7$ films deposited directly on the substrate leads to b and c equal to 187.4 and 0.063, respectively (see the black line corresponding to the mean fit).

ing to $\nu = 1$, 3, 5, and 7, provided that the density of the deposited film is assumed, e.g. 1 g·cm^{-3}.

Results and Discussion

We first investigated the buildup of $(PLL/HA)_m/(PLL/PGA)_n$ films by QCM. Because of the limitation of the penetration of the shear waves used to sense the films, the multilayers should not be too thick (m and n should not exceed 7). It is known that, when built individually, both films, $(PLL/HA)_m$ and $(PLL/PGA)_n$ grow exponentially. We find that this remains true for a $(PLL/PGA)_n$ film built onto a $(PLL/HA)_m$ multilayer (Figure 1). However, one observes that $(PLL/PGA)_n$ grows more rapidly when built on top of $(PLL/HA)_m$ than when deposited on a bare solid substrate. If we fit the evolution of the frequency shift of a $(PGA/PLL)_n$ film deposited on a $(PLL/HA)_6/PLL$ precursor multilayer with an exponential law of the type $-\Delta f/\nu = a + be^{ck}$ where k corresponds to the number of deposited layers ($k = 2n$), the parameter b is equal to 612.0 Hz, and the parameter c is equal to 0.102. These values are to be compared to 131.9 Hz and 0.063 respectively for a $(PLL/PGA)_n$ film deposited on a bare substrate. The parameter b is a measure of the growth of the first few layers until the exponential regime is reached and the parameter c indicates the growth of the subsequent layers within the exponential growth. We hypothesize that the greater value of b observed for the film deposited on the $(PLL/HA)_m$ multilayer is due to PLL and/or PGA chains that are able to diffuse inside the $(PLL/HA)_m$ strata during the initial stages of the $(PLL/PGA)_n$ buildup. This underneath film probably acts as a reservoir for free PLL and/or PGA chains. These free chains, located in the $(PLL/HA)_m$ structure, will contribute to the buildup of the upper PGA/PLL film by diffusing out of the film when it is brought in contact with the PGA solution. They will then interact with the PGA chains of opposite charge at the top of the film. The larger value of c for the two-strata film indicates that the precursor $(PLL/HA)_m$ multilayer also influences the structure of $(PGA/PLL)_n$ film in a way that enhances

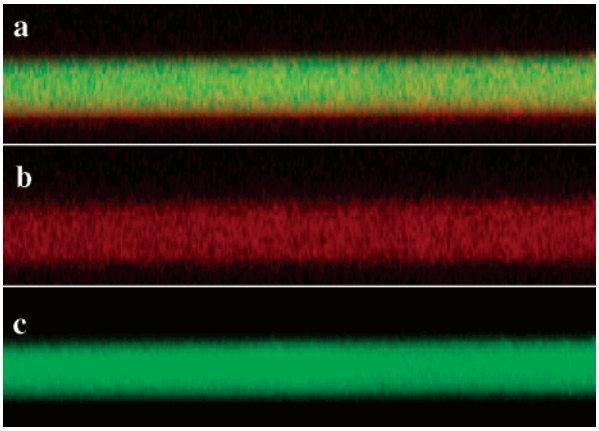

Figure 2. Observation by confocal laser scanning microscopy (CLSM) of the $(PLL/HA)_{30}/PLL^{FITC}/PGA^{AF}$ film section (a) in the red and green channels, (b) in the red channel, and (c) in the green channel. Image sizes are 46.1 × 11.2 μm^2.

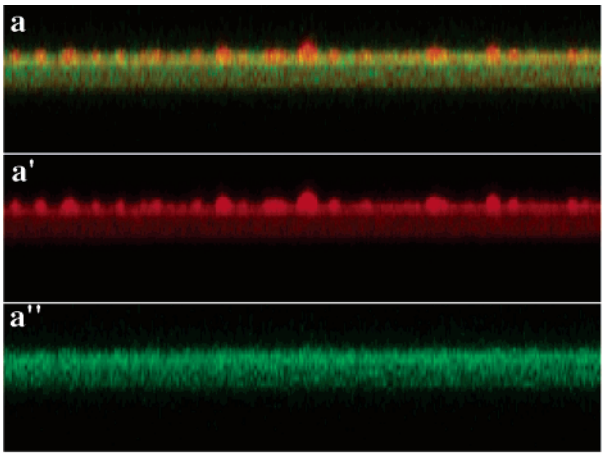

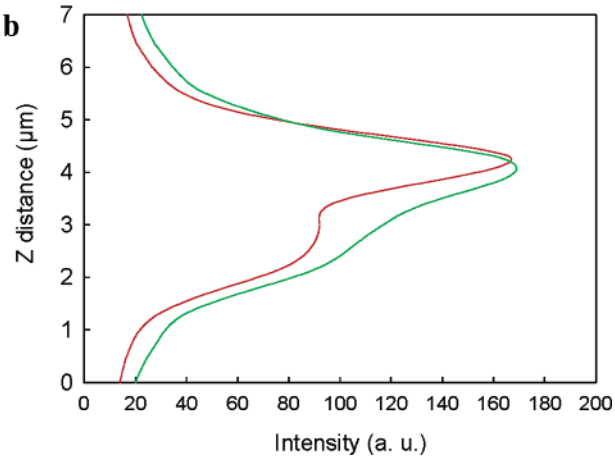

Figure 3. Observation by confocal laser scanning microscopy (CLSM) of the $(PLL/HA)_{30}/PLL^{FITC}/PGA/PLL^{Rho}$ film section (a) in the red and green channel, (a′) in the red channel and (a″) in the green channel. Image sizes are 46.1 × 11.5 μm^2. Fluorescence intensities through the $(PLL/HA)_{30}/PLL^{FITC}/PGA/PLL^{Rho}$ film section (Z distance) are represented in part b. Green and red colors correspond to the fluorescence emission of the PLL^{FITC} and PLL^{Rho}, respectively.

its growth process. This is in marked contrast to what is observed when an exponentially growing film is deposited on a linearly growing one such as $(poly(styrenesulfonate)/poly(allylamine))_n$ which acts similarly to a solid substrate. We also observe that the deposition of a first PGA layer on top of the $(PLL/HA)_m$ film decreases the value of $-\Delta f/\nu$ of the whole film. This can

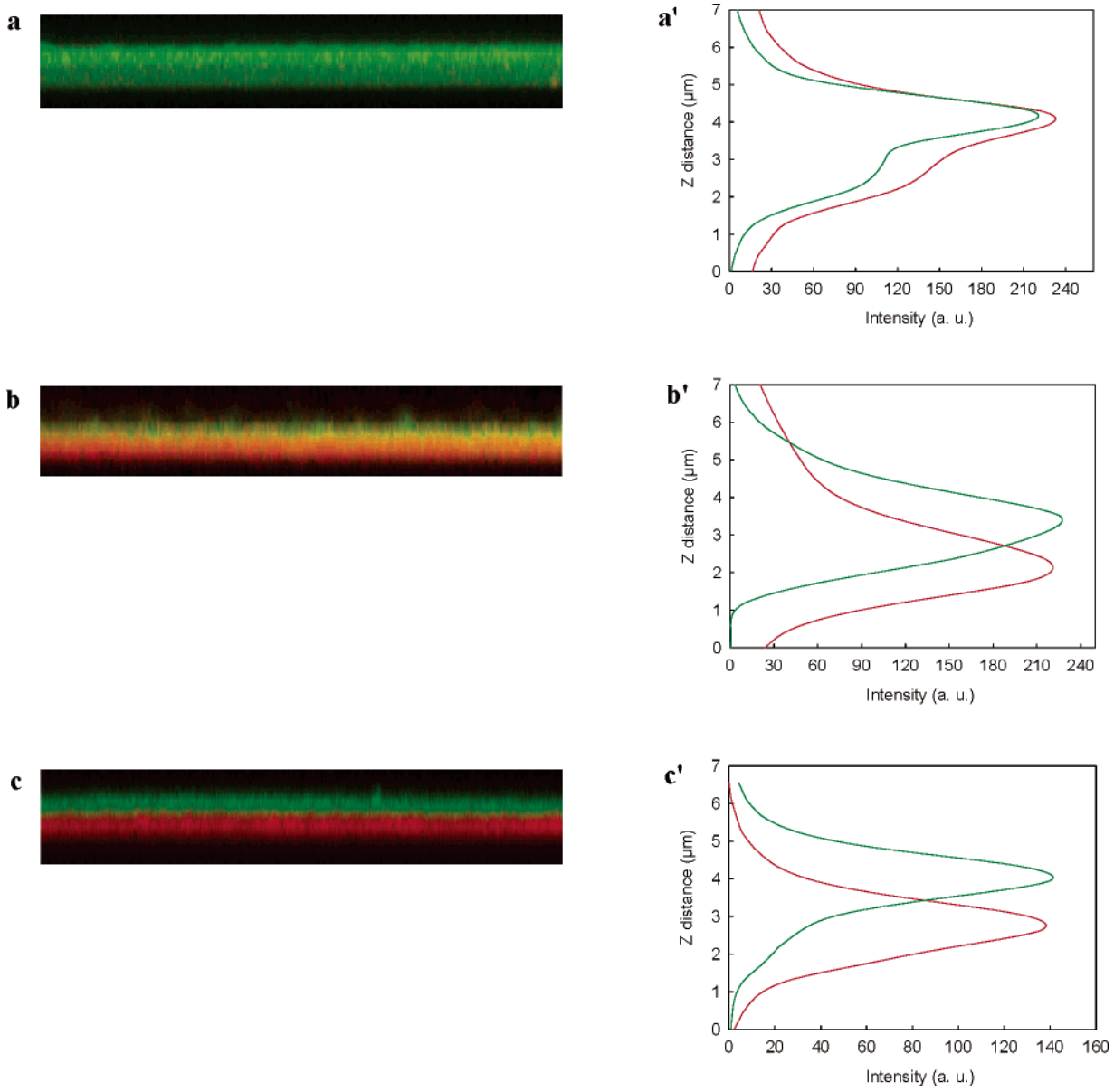

Figure 4. Observation by confocal laser scanning microscopy (CLSM) of the $(PLL/HA)_{30}/PLL^{Rho}/(PGA/PLL)_n/PGA/PLL^{FITC}$ film sections for $n = 0$ (a), $n = 4$ (b) and $n = 10$ (c). Corresponding fluorescence intensity profiles through the film section are displayed in part a′ ($n = 0$), b′ ($n = 4$) and c′ ($n = 10$). Image sizes are $38.6 \times 7\ \mu m^2$. Green and red colors correspond to the fluorescence emission of the PLL^{FITC} and PLL^{Rho}, respectively.

be probably attributed to a loss of water within the film. The thicknesses of the film before and after the first PGA layer deposition calculated from these QCM data are respectively equal to 305 and 163 nm. The deposition of the first PGA layer on top of a $(PLL/HA)_m$ film must lead to a significant shrinking of the precursor multilayer.

We now investigate the ability of PGA and PLL chains deposited on top of a $(PLL/HA)_m$ film during the $(PLL/PGA)_n$ buildup to penetrate into the precursor multilayer. Let us focus on the deposition of the first PGA/PLL bilayer. The shrinking of the $(PLL/HA)_m$ film when brought in contact with the PGA solution suggests that PGA chains diffuse into the underneath $(PLL/HA)_m$ multilayer during the first contact of this film with the PGA solution. Then, the interactions between these PGA chains with the free PLL chains from the film induce its shrinking. To validate the hypothesis of PGA diffusion, we performed CLSM experiments using PGA chains labeled with the Alexa Fluor 594 probe (PGA^{AF}). These chains were brought in contact with a $(PLL/HA)_{30}/PLL^{FITC}$, PLL^{FITC} being used in order to visualize the entire $(PLL/HA)_{30}$ multilayer film. A close look at Figure 2 reveals that the film becomes red and that the red and green colors overlap over almost the whole film section. This validates the hypothesis that the PGA chains brought in contact with the $(PLL/HA)_{30}/PLL^{FITC}$ film diffuse into the entire architecture.

In order to verify if the diffusion of PGA chains into the $(PLL/HA)_m$ structure has changed, the properties of the $(PLL/HA)_{30}/PLL^{FITC}$ multilayer, we performed FRAP experiments. These experiments allow the lateral diffusion of the labeled chains to be sensed. Whereas PLL^{FITC} chains diffuse laterally inside a $(PLL/HA)_{30}/PLL^{FITC}$ over distance of the order of 50 μm over a time scale of 1 h (due to the presence of what we call "free" PLL chains), these chains appear frozen once the $(PLL/HA)_{30}/PLL^{FITC}$ multilayer was brought in contact with a PGA solution: no lateral diffusion could be detected during the time scale of the FRAP experiment. This is a strong indication for the formation of PGA/PLL^{FITC} complexes inside the $(PLL/HA)_{30}/PLL^{FITC}$ multilayer.

Let us now focus our attention on the PLL chains deposited on top of the $(PLL/HA)_{30}/PLL^{FITC}/PGA$ film. For this purpose, we construct a $(PLL/HA)_{30}/PLL^{FITC}/PGA/PLL^{Rho}$ film which is imaged by confocal microscopy. PLL^{FITC} was used to image the precursor $(PLL/HA)_{30}$ multilayer and allows the penetration ability of PLL chains before and after deposition of the first PGA layer to be compared. One observes in Figure 3, parts a, a′, and a″, that the film become entirely green and red, indicating the penetration of both PLL^{FITC} and PLL^{Rho} into the entire film. However, a closer inspection of the vertical sections reveals that the film is not uniformly red but that there is an accumulation of PLL^{Rho} on top of the film. A slight accumulation of PLL^{FITC} on top of the film is also visible but the effect is negligible compared to that of PLL^{Rho}. This accumulation effect is exhibited more rigorously in Figure 3b which represents intensity profiles of the red and green channels. The accumulation of a large fraction of PLL^{Rho} on top of the film can have two non-exclusive origins:

(i) The interactions between PLL and PGA chains can be stronger than between PLL and HA chains. Indeed, we already noticed that PLL^{FITC} deposited on top of a $(PLL/HA)_m$ multilayer can diffuse laterally as observed by FRAP experiment. A similar measurement performed on a $(PLL/PGA)_n$ multilayer reveals that the PLL chains appear frozen in this case, indicating a stronger interaction of PLL with PGA than with HA. It is interesting to notice, in this case that, even though the PLL^{FITC} chains can diffuse into the $(PLL/PGA)_n$ multilayer when a PLL^{FITC} solution is brought in contact with such a film, the chains cannot diffuse laterally inside the film once they have penetrated into the architecture. This is explained by the fact that, once free PLL^{FITC} chains have diffused into the $(PLL/PGA)_n$ multilayer, they probably exchange with nonlabeled PLL chains. The PLL^{FITC} chains become then bound to the film architecture, and it is the immobility of these chains that is detected by FRAP.

(ii) The accumulation of PLL^{Rho} on top of the $(PLL/HA)_{30}/PLL^{FITC}/PGA/PLL^{Rho}$ film could also be due to the fact that after the diffusion of PGA complexes into the $(PLL/HA)_{30}/PLL^{FITC}$ multilayer and the formation of PLL/PGA complexes inside the film, the multilayer becomes more dense and thus hinders partially the diffusion of new PLL chains into the multilayer. This latter hypothesis is supported by the shrinking of the film after contact with the PGA solution, such shrinking being accompanied by a densification of the film.

After the investigation of the effect of the deposition of the first PGA/PLL bilayer on the underneath $(PLL/HA)_m$ film, we have focused our attention on the $(PLL/HA)_{30}/PLL^{Rho}/(PGA/PLL)_n/PGA/PLL^{FITC}$ multilayers with n equal to 4 and 10. For each film, we have determined the intensity profiles in the green and red channels. Figure 4 shows the evolution of the film sections taken by confocal microscopy and the evolution of the corresponding intensity profiles for $n = 0$, $n = 4$ and $n = 10$. One first observes that PLL^{FITC} continues to diffuse into the film for $n = 4$ (Figure 4, parts b and b′) as was the case for $n = 0$ (Figure 4, parts a and a′; see also Figure 3). However, the overlap between the green and red colors diminishes as n increases. This indicates that while PLL^{FITC} diffuses into the $(PLL/PGA)_n$ upper multilayer, the fraction of PLL^{FITC} chains present in the entire film that diffuse into the underneath $(PLL/HA)_m$ multilayer decreases. Whereas for $n = 4$ a small fraction of the PLL^{FITC} chains deposited on top of the film still seems to penetrate in the $(PLL/HA)_m$ zone, this seems no longer to be the case for $n = 10$ (Figure 4, parts b and b′). The slight overlap between the two fluorescent stripes is probably due to limitation in CLSM resolution (around 500 nm in the Z direction). For $n = 10$, the PLL^{Rho} and PLL^{FITC} are thus probably mainly located respectively in the $(PLL/HA)_{30}$ and in the $(PGA/PLL)_{10}$ strata. Finally, using FRAP experiments performed on $(PLL/HA)_{30}/PLL^{FITC}/(PGA/PLL)_n/PGA/PLL^{Rho}$ films, we checked that the PLL^{FITC} chains lost totally they lateral diffusion ability in the $(PLL/HA)_{30}$ multilayer. By interchanging the dyes (PLL^{FITC} by PLL^{Rho} and PLL^{Rho} by PLL^{FITC}), we verified that this loss of diffusion is not an effect of the dyes but an intrinsic property of the films.

Conclusions

To conclude, we demonstrate that an exponentially growing film, namely $(PLL/PGA)_n$, can be built on top of another exponentially growing film, namely$(PLL/HA)_m$, and that the growth process of the upper film remains exponential. When a first PGA/PLL bilayer is deposited on top of the $(PLL/HA)_m$ film, both PLL and PGA diffuse into the entire $(PLL/HA)_m$ architecture. The penetration of the PGA chains into the underneath $(PLL/HA)_m$ architecture leads to the formation of PGA/PLL complexes inside the HA/PLL multilayer. At the same time the film shrinks and becomes more dense. This process further inhibits the diffusion of the PLL chains from the $(PLL/HA)_m$ architecture, and the chains appear as frozen. One can expect that this overall process goes on during the first PGA/PLL deposition steps leading to an increase of the density of the $(PLL/HA)_m$ multilayer. After several deposition steps, the densification of the underneath film is such that it greatly suppresses penetration of PLL chains.

These results are of main importance for the design of multifunctional bioactive films whose activity is scheduled in time. This could be of interest, for example, in tissue engineering, where different growth factors acting at different evolution stages could be embedded in substrata films.

Acknowledgment. This work was supported by the ACI "Nanosciences 2004" from the Ministère de la Recherche et des Nouvelles Technologies (Project NR204). Ph. L is indebted to Hôpitaux Universitaires de Strasbourg for financial support. We thank Jérôme Mutterer (Institut de Biologie Moléculaire des Plantes, CNRS/ULP, Strasbourg, France) and Sylvette Chasserot-Golaz (Centre de Neurochimie, INSERM/CNRS/ULP, Strasbourg, France), for their helps with the CLSM. The CLSM platform used in this study was co-financed by the Région Alsace, the Université Louis Pasteur, and the Association pour la Recherche sur le Cancer. We also thank Karim Benmlih for his technical assistance.

References and Notes

(1) Decher, G.; Hong, J. D.; Schmitt, J. Buildup of ultrathin multilayer films by a self-assembly process. Consecutively alternating adsorption of anionic and cationic polyeletrolytes on charges surface. *Thin Solid Films* **1992**, *210*, 831−835.
(2) Decher, G. Fuzzy nanoassemblies: Toward layered polymeric multicomposites. *Science* **1997**, *277*, 1232−1237.
(3) Iler, R. *J. Colloid Interface Sci.* **1966**, *21*, 569.
(4) Thierry, B.; Winnik, F. M.; Merhi, Y.; Tabrizian, M. Nanocoatings onto arteries via layer-by-layer deposition: Toward the in vivo repair of damaged blood vessels. *J. Am. Chem. Soc.* **2003**, *125*, 7494−7495.
(5) Tang, Z. Y.; Kotov, N. A.; Magonov, S.; Ozturk, B. Nanostructured artificial nacre. *Nat. Mater.* **2003**, *2*, 413−418.
(6) Radt, B.; Smith, T. A.; Caruso, F. Optically addressable nanostructured capsules. *Adv. Mater.* **2004**, *16*, 2184−2189.
(7) Thierry, B.; Faghihi, S.; Torab, L.; Pike, G. B.; Tabrizian, M. Magnetic resonance signal-enhancing self-assembled coating for endovascular devices. *Adv. Mater.* **2005**, *17*, 826−830.
(8) Schultz, P.; Vautier, D.; Richert, L.; Jessel, N.; Haikel, Y.; Schaaf, P.; Voegel, J.-C.; Ogier, J.; Debry, C. Polyelectrolyte multilayers

functionalized by a synthetic analogue of an anti-inflammatory peptide, alpha-MSH, for coating a tracheal prosthesis. *Biomaterials* **2005**, *26*, 2621−2630.
(9) Etienne, O.; Picart, C.; Taddei, C.; Haikel, Y.; Dimarcq, J. L.; Schaaf, P.; Voegel, J.-C.; Ogier, J. A.; Egles, C. Multilayer polyelectrolyte films functionalized by insertion of defensin: A new approach to protection of implants from bacterial colonization. *Antimicrob. Agents Chemother.* **2004**, *48*, 3662−3669.
(10) Jewell, C. M.; Zhang, J.; Fredin, N. J.; Lynn, D. M. Multilayered polyelectrolyte films promote the direct and localized delivery of DNA to cells. *J. Controlled Release* **2005**, *106*, 214−223.
(11) Lynn, D. M. Layers of opportunity: nanostructured polymer assemblies for the delivery of macromolecular therapeutics. *Soft Matter* **2006**, *2*, 269−273.
(12) Hammond, P. T. Form and function in multilayer assembly: New applications at the nanoscale. *Adv. Mater.* **2004**, *16*, 1271−1293.
(13) Liu, X. Y.; Bruening, M. L. Size-selective transport of uncharged solutes through multilayer polyelectrolyte membranes. *Chem. Mater.* **2004**, *16*, 351−357.
(14) Cortez, C.; Tomaskovic-Crook, E.; A. P. R.; J.; Radt, B.; Cody, S. H.; Scott, A. M.; Nice, E. C.; Heath, J. K.; Caruso, F. Targeting and Uptake of Multilayered Particles to Colorectal Cancer Cells. *Adv. Mater.* **2006**, *18*, 1998−2003.
(15) Shchukin, D. G.; Kohler, K.; Möhwald, H. Microcontainers with electrochemically reversible permeability. *J. Am. Chem. Soc.* **2006**, *128*, 4560−4561.
(16) Mendelsohn, J. D.; Yang, S. Y.; Hiller, J.; Hochbaum, A. I.; Rubner, M. F. Rational Design of Cytophilic and Cytophobic Polyelectrolyte Multilayer Thin Films. *Biomacromolecules* **2003**, *4*, 96−106.
(17) Sukhorukov, G. B.; Schmitt, J.; Decher, G. Reversible swelling of polyanion/polycation multilayer films in solutions of different ionic strength. *Ber. Bunsen-Ges. Phys. Chem* **1996**, *100*, 948−953.
(18) Ladam, G.; Schaad, P.; Voegel, J.-C.; Schaaf, P.; Decher, G.; Cuisinier, F. In situ determination of the structural properties of initially deposited polyelectrolyte multilayers. *Langmuir* **2000**, *16*, 1249−1255.
(19) McAloney, R. A.; Sinyor, M.; Dudnik, V.; Goh, M. C. Atomic force microscopy studies of salt effects on polyelectrolyte multilayer film morphology. *Langmuir* **2001**, *17*, 6655−6663.
(20) Ruths, J.; Essler, F.; Decher, G.; Riegler, H. Polyelectrolytes I: Polyanion/Polycation Multilayers at the Air/Monolayer/Water Interface as Elements for Quantitative Polymer Adsorption Studies and Preparation of Hetero-superlattices on Solid Surfaces. *Langmuir* **2000**, *16*, 8871−8878.
(21) Sukhishvili, S. A. Responsive polymer films and capsules via layer-by-layer assembly. *Curr. Opin. Colloid Interface Sci.* **2005**, *10*, 37−44.
(22) Shiratori, S. S.; Rubner, M. F. pH-Dependent Thickness Behavior of Sequentially Adsorbed Layers of Weak Polyelectrolytes. *Macromolecules* **2000**, *33*, 4213−4219.
(23) Elbert, D. L.; Herbert, C. B.; Hubbell, J. A. Thin polymer layers formed by polyelectrolyte multilayer techniques on biological surfaces. *Langmuir* **1999**, *15*, 5355−5362.
(24) Picart, C.; Mutterer, J.; Richert, L.; Luo, Y.; Prestwich, G. D.; Schaaf, P.; Voegel, J.-C.; Lavalle, P. Molecular basis for the explanation of the exponential growth of polyelectrolyte multilayers. *Proc. Natl. Acad. Sci. U.S.A.* **2002**, *99*, 12531−12535.
(25) Boulmedais, F.; Ball, V.; Schwinté, P.; Frisch, B.; Schaaf, P.; Voegel, J.-C. Buildup of exponentially growing multilayer polypeptide films with internal secondary structure. *Langmuir* **2003**, *19*, 440−445.
(26) DeLongchamp, D. M.; Hammond, P. T. Fast ion conduction in layer-by-layer polymer films. *Chem. Mater.* **2003**, *15*, 1165−1173.
(27) Schoeler, B.; Poptoshev, E.; Caruso, F. Growth of multilayer films of fixed and variable charge density polyelectrolytes: effect of mutual charge and secondary interactions. *Macromolecules* **2003**, *36*, 5258−5264.
(28) Salomaki, M.; Vinokurov, I. A.; Kankare, J. Effect of temperature on the buildup of polyelectrolyte multilayers. *Langmuir* **2005**, *21*, 11232−11240.
(29) Halthur, T. J.; Elofsson, U. M. Multilayers of charged polypeptides as studied by in situ ellipsometry and quartz crystal microbalance with dissipation. *Langmuir* **2004**, *20*, 1739−1745.
(30) Porcel, C.; Lavalle, P.; Ball, V.; Decher, G.; Senger, B.; Voegel, J.-C.; Schaaf, P. From exponential to linear growth in polyelectrolyte multilayers. *Langmuir* **2006**, *22*, 4376−4383.
(31) Picart, C.; Mutterer, J.; Arntz, Y.; Voegel, J.-C.; Schaaf, P.; Senger, B. Application of fluorescence recovery after photobleaching to diffusion of a polyelectrolyte in a multilayer film. *Microsc. Res. Technol.* **2005**, *66*, 43−57.
(32) Lavalle, P.; Vivet, V.; Jessel, N.; Decher, G.; Mesini, P. J.; Voegel, J.-C.; Schaaf, P. Direct evidence for vertical diffusion and exchange processes of polyanions and polycations in polyelectrolyte multilayer films. *Macromolecules* **2004**, *37*, 1159−1162.
(33) Jessel, N.; Atalar, F.; Lavalle, P.; Mutterer, J.; Decher, G.; Schaaf, P.; Voegel, J.-C.; Ogier, J. Bioactive coatings based on a polyelectrolyte multilayer architecture functionalized by embedded proteins. *Adv. Mater.* **2003**, *15*, 692−695.
(34) Jessel, N.; Oulad-Abdeighani, M.; Meyer, F.; Lavalle, P.; Haikel, Y.; Schaaf, P.; Voegel, J.-C. Multiple and time-scheduled in situ DNA delivery mediated by beta-cyclodextrin embedded in a polyelectrolyte multilayer. *Proc. Natl. Acad. Sci. U.S.A.* **2006**, *103*, 8618−8621.
(35) Garza, J. M.; Schaaf, P.; Muller, S.; Ball, V.; Stoltz, J.-F.; Voegel, J.-C.; Lavalle, P. Multicompartment films made of alternate polyelectrolyte multilayers of exponential and linear growth. *Langmuir* **2004**, *20*, 7298−7302.
(36) Garza, J. M.; Jessel, N.; Ladam, G.; Dupray, V.; Muller, S.; Stoltz, J.-F.; Schaaf, P.; Voegel, J.-C.; Lavalle, P. Polyelectrolyte multilayers and degradable polymer layers as multicompartment films. *Langmuir* **2005**, *21*, 12372−12377.
(37) Hermanson, G. T. In *Bioconjugate techniques*; Hermanson, G. T., Ed.; Academic Press: San Diego, CA, 1996; pp 169−176.
(38) Zhang, J.; Senger, B.; Vautier, D.; Picart, C.; Schaaf, P.; Voegel, J.-C.; Lavalle, P. Natural polyelectrolyte films based on layer by layer deposition of collagen and hyaluronic acid. *Biomaterials* **2005**, *26*, 3353−3361.
(39) Voinova, M. V.; Rodahl, M.; Jonson, M.; Kasemo, B. Viscoelastic acoustic response of layered polymer films at fluid-solid interfaces : continuum mechanics approach. *Phys. Scr.* **1999**, *59*, 391−396.

MA062201E